**IN: PHOTONIC ELECTRONIC AND ATOMIC COLLISIONS**
**PROCEEDINGS OF THE ICPEAC 2001, RINTON PRESS**

# DOUBLE IONIZATION IN STRONG LASER FIELDS

R. DÖRNER, TH. WEBER, M. WECKENBROCK, A. STAUDTE, S. KAMMER,
H. SCHMIDT-BÖCKING
*Institut für Kernphysik August Euler Str. 6 60486 Frankfurt, Germany*
*E-mail: doerner@hsb.uni-frankfurt.de*

H. ROTTKE
*Max-Born-Institut, Rudower Chausse 6, 12489 Berlin, Germany*

R. MOSHAMMER, B. FEUERSTEIN, J. ULLRICH
*Max-Planck-Institut für Kernphysik Saupfercheckweg 1 69117 Heidelberg, Germany*

In strong laser fields ($10^{14} - 10^{15} W/cm^2$, 800nm) all atoms have a high probability to become singly or even multiply ionized. These ionization processes can be studied in great detail by imaging the momenta of the resulting ions and electrons with COLTRIMS (Cold Target Recoil Ion Momentum Spectroscopy). The momenta of the ions give a direct insight in the role of electron correlation during the ionization process. They strongly support a rescattering scenario in which first one electron couples to the field is finally driven back to its parent ion and tranfers the energy to the second electron. A double peak structure found in the ion momentum distribution gives a direct measure of the time delay introduced by the rescattering trajectory. The two electrons are finally found to be emitted with similar momentum to the same hemisphere. These results are compared to double ionization by charged particle and single photon impact.

## 1 Atoms in strong fields

70 years ago Maria Göppert-Mayer [1] showed that the energy of many photons can be combined to achieve ionization in cases where the energy of one photon is not sufficient to overcome the binding. Modern short pulse Ti:Sa lasers (800nm, 1.5eV) routinely provide intensities of more than $10^{16} W/cm^2$ and pulses shorter than 100 femto seconds. Under these conditions the ionization probability of most ions is close to unity. $10^{16} W/cm^2$ corresponds to about $10^{10}$ coherent photons in a box of the size of the wavelength (800nm). This high density of photons is necessary to allow for such highly nonlinear multiphoton absorption.

The high density of coherent photons in the laser pulse also suggests a change from the "photon-" to the "field-perspective" : the laser field can be described as a classical electromagnetic field, neglecting the quantum nature of the photons. From this point of view the relevant quantity is the field strength. $10^{16} W/cm^2$ at 800 nm corresponds to a field of $3 \times 10^{11} V/m$.

*Single ionization* in such strong fields has been intensely studied for many years now. The experimental observables are the ionization rates as function of laser intensity and wavelength, the electron energy and angular distribution as well as the emission of higher harmonic light. We refer the reader to excellent review articles covering this exciting and rich field [2,3].

The present article focuses on some recent advances in unveiling the mechanism of *double and multiple ionization* in strong fields. Since more particles are involved the number of observables and the challenge to the experimental techniques increases. Early studies

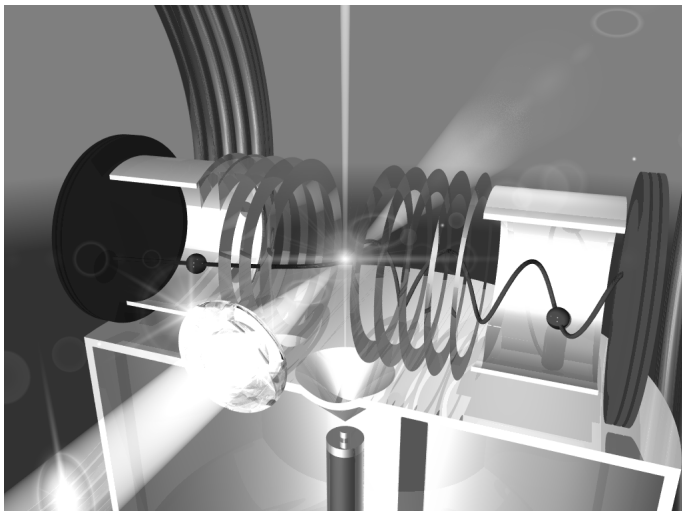

Figure 1. Experimental setup. Electrons and ions are created in the supersonic gas jet target. The thin copper rings create a homogeneous electric field, the large Helmoltz coils an additional magnetic field. These fields guide the charged particles onto fast time and position sensitive channel plate detectors (Roentdek www.roentdek.com). Time-of-flight and position of impact of each electron-ion pair is recorded in list mode. From this the three dimensional momentum vector of each particle can be calculated.

measured the rate of highly charged ions as function of laser intensity. The work reviewed here employs COLTRIMS (Cold Target Recoil Ion Momentum Spectroscopy)[4] to detect not only the charge state but also the momentum vector of the ion and one of the electrons in coincidence. Such highly differential measurements are standard today in the fields of ion-atom-, electron-atom- and high energy single photon-atom-collision studies.

The main question discussed in the strong field case is the role of electron correlation in the multiple ionization process. Do the electrons escape from the atom sequentially or nonsequentially? Does each electron absorb the photons independently, or does one electron absorb the energy from the field and then share it with the second electron via electron-electron correlation?

## 2 COLTRIMS – a cloud chamber for atomic physics

COLTRIMS is an imaging technique which measures the momenta and charge states of all charged fragments from an atomic or molecular fragmentation process in coincidence. A typical setup as it was used for the experiments discussed here is shown in figure 1. The laser pulse is focused by a lens of 5cm focal length or a parabolic mirror into a supersonic gas-jet. The gas-jet provides target atoms with very small initial momentum spread of below 0.1 a.u. (atomic units) in the direction of the laser polarization. For experiments in ion-atom collisions or with synchrotron radiation the ionization probability is very small and hence, one aims at a target density in the range of up to $10^{-4}$mbar local pressure in the gas-jet. Accordingly for such experiments a background pressure in the chamber in the range of $10^{-8} mbar$ is sufficient. In these experiments the volume in which the reaction occurs is given

by the overlap of the photon or ion beam with the gas-jet, which is typically $0.1 - 1mm^3$. For ionization by femto second laser pulses in contrast the reaction volume is defined by the laser focus typically $10\mu$m $\times$ $100\mu$m. Within this volume the ionization probability can, however, reach unity. Since for coincidence experiments it is essential that much less than one atom is ionized per laser shot a background pressure of $< 10^{-10}$mbar is required. The gas-jet has to be adjusted accordingly to reach single collision conditions at the desired laser peak power. With standard super sonic gas-jets this is not easily achieved, since a lower driving pressure for the expansion results in an increase of the internal temperature of the jet along its direction of propagation.

The ions created in the laser focus are guided by a weak electric field towards a position sensitive channel plate detector. From the position of impact and the time of flight of the ion all three components of the momentum vector and the charge state are obtained. The electric field also guides the electrons towards a second position sensitive channel plate detector. To collect electrons with higher energy a homogeneous magnetic field is superimposed parallel to the electric field. This guides the electrons on cyclotron trajectories towards the detector [5]. From the measured time-of-flight and the position of impact these trajectories can be reconstructed and the starting momentum can be uniquely calculated for most cases. Using a magnetic field of 10 Gauss $4\pi$ solid angle collection is achieved for electrons up to about 30eV. The typical detection probability of an electron is in the range of 30% (given by the channel plate open area and the transmission of the grids in the spectrometer). Thus even for double ionization in most cases only one electron is detected. The positions of impact and the times-of-flight are stored for each event in list mode. Thus the whole experiment can be replayed in the offline analysis.

## 3 Single ionization and the two-step model

The momentum distribution of singly charged helium ions produced by absorption of one 80eV photon (synchrotron radiation) and by multiphoton absorption at 800nm $1.3 \times 10^{15}$ W/cm$^2$ is shown in fig. 2. In both cases the momentum of the photon is negligible compared to the electron momentum. Therefore electron and $He^{1+}$ ion are emitted back to back compensating each others momentum. For single ionization the spectroscopy of the ion momentum is hence equivalent to electron spectroscopy.

For single photon absorption the electron energy is uniquely determined by the photon energy $E_\gamma$ and the binding energy plus a possible internal excitation energy of the residual ion. The resulting narrow lines in the photo electron energy spectrum correspond to spheres in momentum space. The left panel of fig. 2 shows a slice through this momentum sphere. The outer ring corresponds to $He^{1+}$ ions in the ground state, the inner rings to the excited states. The photons are linearly polarized with the polarization horizontal. The angular distribution of the outer ring shows an almost pure dipole distribution. Contrary, in the laser field any number of photons can be absorbed, leading to an almost continuous electron energy distribution of the electrons. The structure of ATI (above threshold ionization) individual peaks spaced by the photon energy (1.5 eV) is not resolved here. The electrons and ions are emitted in narrow jets along the polarization axis. Such high angular momentum states are accessible due to the high number of photons absorbed.

How do the ions and electrons get their momentum? For the case of single photon absorption the light field is so weak that there is no external acceleration. Also the photon

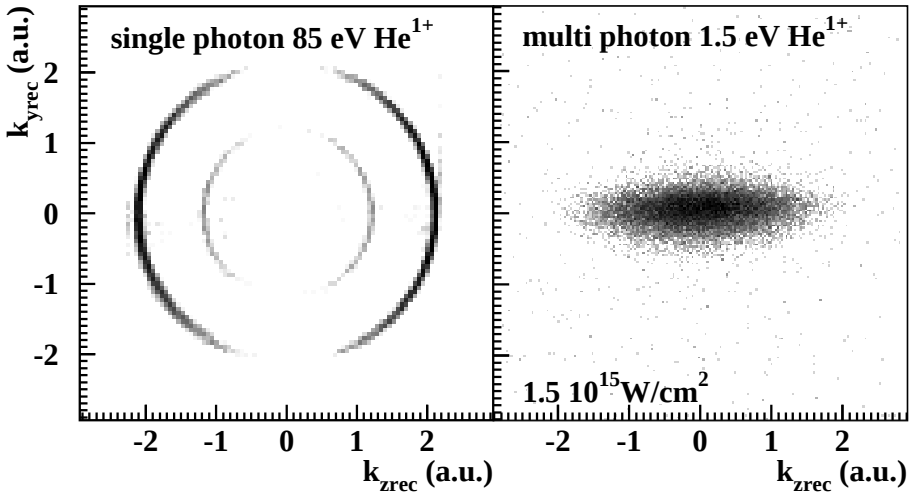


Figure 2. Momentum distribution of $He^{1+}$ ions. Left: For 85 eV single photon absorption. Right: 1.5 eV (800nm), 220 fsec, $1.4 \times 10^{15}$ W/cm$^2$. The polarization vector of the light is horizontal. The photon momentum is vertical. In the left figure the momentum component in the third dimension out of the plane of the figure is restricted to $\pm 0.4 a.u.$, the right panel is integrated over the momenta in the direction out of the plane of the figure.

carries no significant momentum into the reaction. The momenta observed in the final state thus have to be present already in the initial state of the atom. The photon cuts the tie between nucleus and electron by providing the energy, the momentum however was present already in the initial state Compton profile. Single photon absorbtion is therefore linked to a particular fraction of the initial state wave function which in momentum representation concides with the final state momentum. In the coordinate space representation this fraction of the wave function is confined close to the nucleus. The scaling of the photo ionization cross section at high energies simply follows the initial state momentum space Compton profile, i.e. the probability to find an electron-ion pair with the appropriate momentum in the initial state. In the strong field case the situation changes completely. The field is strong enough to accelerate the ions and electrons substantially after the electron is set free. The momentum balance however is still the same as in the single photon limit: The laser field accelerates electron and ion to the opposite directions resulting again in their back-to-back emission. Only if the laser pulse is long enough that the electron can escape from the focus during pulse duration this changes. In this case, which we do not consider here, the momenta are balanced by a huge amount of elastically scattered photons. In the regime of wavelength and binding energies under consideration here, a simple two-step picture has been proven useful. In the first step the electron is set free by tunneling through the potential barrier created by the superposition of the coulomb potential of the atom and the electric field of the laser. This process promotes electrons and ions with zero momentum to the continuum. They are then accelerated in the laser field and perform a quiver motion.

The net momentum which is observed after the pulse with envelope of the electric field strength E(t) is in this model purely a function of the phase of the field at the instant of tunneling (tunneling time $t_0$) (atomic units are used throughout this paper):

$$p_z^{He^{1+}}(t_\infty) = \int_{t_0}^{t_\infty} E(t) \sin \omega t dt \tag{1}$$

Tunneling at the field maximum thus leads to electrons and ions with zero momentum. The maximum momentum corresponding to the zero crossing of the laser field is $\sqrt{4U_p}$, where $U_p = I/4\omega^2$ is the ponderomotive potential at an intensity I and the photon frequency $\omega$ ($U_P$ =39.4 eV at $6.6{\cdot}10^{14}$W/cm$^2$).

Single ionization is shown here mainly for illustration. Much more detailed experiments have been reported using conventional time-of-flight electron spectrometers (see [3] and references therein).

## 4 Mechanisms of double ionization

What are the mechanisms leading to double ionization? This seemingly clear-cut question does not necessarily have a quantum mechanical answer. The word mechanism mostly refers to an intuitive mechanistical picture. It is not always clear how this intuition can be translated into a theory and even if one finds such a translation the contributions from different mechanism have to be added coherently [6,7] to obtain the measurable final state of the reaction. Thus only in some cases mechanisms are experimentally accessible. This is only the case if different mechanisms occur at different strength of the perturbation (such as laser power or projectile charge) or if they populate different regions of final state phase space. With these words of caution in mind, we list the most discussed mechanisms leading to double ionization:

1. **TS2 or Sequential Ionization:** Here the two electrons are emitted sequentially by two independent interactions of the laser field with the atom. From a photon perspective one could say that each of the electrons absorbs photons independently. From the field perspective one would say that each electron tunnels independently at different times during the laser pulse. This is equivalent to the TS2 (two-step-two) mechanism in ion-atom and electron-atom collisions. In this approximation the probability of double ejection can be estimated in an independent particle model. Most simply one calculates double ionization as two times independent single ionization. A little more refined approach uses an independent event model, which takes into account the different binding energies for ejection of the first and the second electron (see e.g. [8] for ion impact, [9] for laser impact).

2. **Shake Off:** If one electron is removed rapidly (sudden approximation) from an atom or a molecule, the wave function of the remaining electrons has to relax to the new eigenstates of the altered potential. Part of these states are in the continuum, so that a second electron can be "shaken off" in this relaxation process. This is known for example from beta decay where the nuclear charge is changed. Shake off is also known to be one of the mechanisms for double ionization by absorption or Compton scattering of a single photon (see the discussion in [10] and references therein). Only for very high photon energies (keV) it is however the dominating mechanism for double

ionization. For Helium it leads to a ratio of double to single ionization of 1.66% [11,12] for photoabsorption (emission of the first electron from close to the nucleus) and 0.86% for Compton scattering (averaged over the initial state Compton profile) [13].

3. **Two-Step-One (TS1):** For single photon absorption at lower photon energies (threshold to several 100eV [7]) TS1 is known to dominate by far over the shake off contribution. A simplified picture of TS1 is that one electron absorbs the photon and knocks out the second one via an electron-electron collision on its way through the atom [14]. A close connection between the electron impact ionization cross section and the ratio of double to single ionization by single photon absorption as function of the energy is seen experimentally [14] and theoretically [7], supporting this simple picture. For the TS1 mechanism the electron correlation is on a very short time scale (a few attoseconds) and confined to the small region of space (the size of the electron cloud).

4. **Rescattering:** Rescattering is a version of the TS1 mechanism which is induced only by the laser field. The mechanism was proposed originally by Kuchiev[15] under the name "antenna model". He suggested that one of the electrons is driven in the laser field acting as an antenna absorbing the energy which it then shares with the other electron via correlation. Corkum[16] and Schafer[17] extended this basic idea and interpreted the process in the two step model: First one electron is set free by tunneling. It is accelerated by the laser field and is in half of the cases driven back to its parent ion. Upon recollision with the ion the electron can recombine and emit higher harmonic radiation, it can be elastically scattered and be further accelerated and it can also be inelastically scattered and excite or further ionize the ion. In contrast to TS1 in this case there is a femto second time delay between the first and the second step. Also the wave function of the rescattered electron explores a larger region of space [18,19] as in the case of TS1.

A distinction between sequential ionization on one side and all the nonsequential processes on the other must be present. A strong experimental evidence favouring the rescattering process was later provided by the observation that double ionization is strongly suppressed in circularly polarized light[20]. The rescattering mechanism is inhibited by the circular polarization since the rotating electric field does not drive the electrons back to their origin, while in contrast the other mechanisms are expected to be polarization independent.

To gain further insight in the double ionization process clearly differential measurements beyond the ion yield are necessary. In addition to such experiments performed recently with COLTRIMS described here two other groups also succeded in electron time-of-flight measurements in coincidence with the ion charge state [21,22].

## 5 Recoil ion momenta

The recoil ion is an important messenger carrying detailed information on the time evolution of the ionization process. In analogy to the situation for single ionization discussed above one can estimate the net momentum accumulated by the doubly charged ion from the laser pulse as

$$p_z^{He^{2+}}(t_\infty) = \int_{t_1}^{t_{12}} E(t)\sin\omega t dt + 2\int_{t_{12}}^{t_\infty} E(t)\sin\omega t dt. \qquad (2)$$

The first electron is removed at time $t_1$ and the ion switches its charge from $1^+$ to $2^+$ at time $t_{12}$. It is assumed that there is no momentum transfer to the ion from the electron. Thus as in the case of single ionization the phase of the field at the instant of the emission of the first and of the second electron is encoded in the ion momentum. For the TS2 mechanism one has for example two sequential steps of single ionization, each of them most likely at the field maximum. Thus TS2 (or sequential ionization) will produce a peak in the ion momentum at zero and the distribution will be given by the distribution for single ionization convoluted with itself (see [23] for the case of Ar). For the shake off process the emission of the second electron will follow extremely fast (much faster than a laser cycle) after the emission of the first electron, thus $t_1 = t_{12}$ in equation 2. Again this will lead to a maximum at zero momentum, like in single ionization. The experimental distribution however shows a distinct double peak structure for Helium[24] as well as for Neon[25] (see fig. 3). *This can be understood as a result of the time delay due to the rescattering of the first electron.* Estimating $t_{12}$ for a rescattering trajectory which has sufficient energy to ionize leads to momenta close to the measured peak position [24,25,26]. The high momenta of the doubly and triply charged ions are direct proof of the time delay introduced by the rescattering trajectory. It is this time delay with respect to the field maximum with which the ion switches its charge, which allows an effective net momentum transfer to the ion.

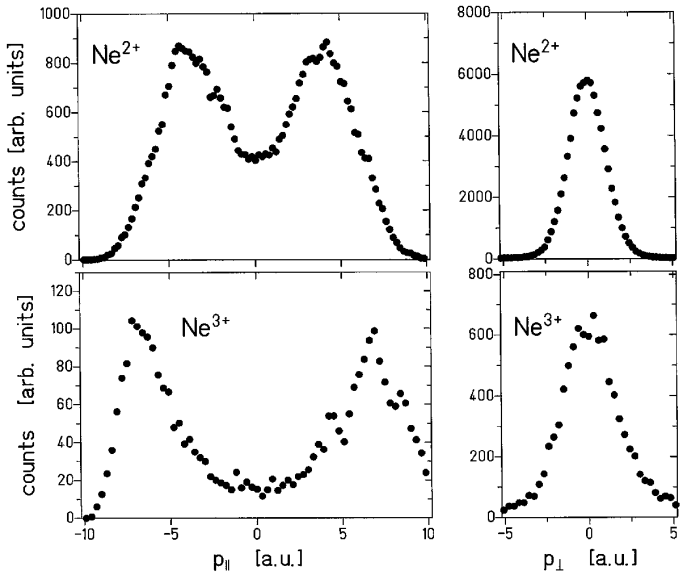


Figure 3. Momentum distribution of $Ne^{2+}$ and $Ne^{3+}$ ions produced at $1.3\times10^{15}W/cm^2$ ($Ne^{2+}$) and $1.5\times10^{15}W/cm^2$ ($Ne^{3+}$). $p_\parallel$ is the componentne parallel to the laser polarization, $p_\perp$ perpendicular to it (from [25])

More quantitatively ion momenta for helium have been calculated within the S-Martix theory by A.Becker and F.H. Faisal [27] yielding good agreement with experimental data. They could show that the ion momenta are produced in the field after the emission of the

second electron. These conclusions could be confirmed in S-Matrix calculation for Neon[28] and in Wannier type calculations[29]. Lein et al.[19] solved the time dependend Schrödinger equation in one dimension and Chen et al.[30] have performed a Classical Trajectory Monte Carlo calculation in which they solved the classical Hamilton equations of motion initializing one electron by tunneling. Both calculations could reproduce the observed double peak structure.

## 6 Correlated Electron Momenta

For double ionization by single photon absorption it is known that in the final state the effect of electron repulsion strongly suppresses emission to the same hemisphere (see e.g. figure 5 in [31]). For double ionization by heavy ion impact (which can be viewed as an attosecond half cycle pulse) also emission of both electrons is found preferentially to opposite sides[32]. Recent experiment on double ionization by electron impact also confirm this influence of electron repulsion [33]. All these double ionization processes have in common that there is no strong external field active in the final state. For double ionization in the laser field this is very different, the field is present long after the electrons are in the continuum. This changes the electron emission completely.

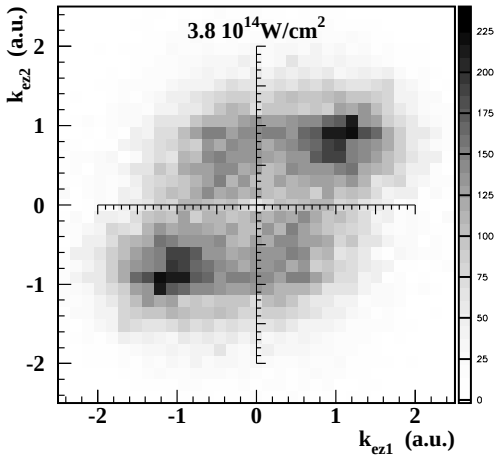


Figure 4. Momentum correlation between the two emitted electrons when a $Ar^{2+}$ ion is produced in the focus of a 220 fsec, 800nm laser pulse at peak intensities of $3.8 \cdot 10^{14}$ W/cm$^2$. The horizontal axis shows the momentum components of one electron along the polarization of the laser field, the vertical axis the same momentum component of the corresponding second electron. Same sign of the momenta for both electrons means emission to the same half sphere. The data are integrated over the momentum components in the direction perpendicular to the polarization. The grey shading shows the differential rate in arbitrary units (adapted from [34]).

Fig. 4 shows the momentum correlation between the two electrons emitted from an argon atom at a laser intensity where nonsequential ionization dominates. A distinct maximum

for both electrons traveling to the same side with similar momentum is found. Obviously the action of the laser field on the electrons determine their final momenta. It is the laser field which drives both electrons to the same side, counteracting electron repulsion. For a detailed comparison with single photon absorption see [35]. The position of the maximum is in agreement with the expectation from the rescattering model if one takes excited intermediated states into account (see [34,36,37,38,39] for a more detailed analysis).

## 7 Outlook

The application of COLTRIMS has yielded the first differential data for double ionization in strong laser fields. Compared to the experimental situation in double ionization by single photon absorption, however, the experiments are still in their infancy. So far correlated electron momenta have been measured only for Argon and Neon. Clearly experiments on Helium are highly desirable since this is where theory is most tractable. Also the experiments so far have mainly investigated the momentum component in the polarization direction. Only most recently the influence of the transverse momentum of one of the electrons has been investigated for Argon [36]. Similar results for Neon are in preparation. These are however not yet fully differential data since not all 6 momentum components of the two electrons are analyzed. Therefore, no coincident angular distributions as for single photon absorption are available at this point (see[40] for a theoretical prediction of these distributions). Most important for such future studies is a high energy resolution of the sum energy of the two electrons, which would allow to count the number of photons absorbed. From single photon absorption it is known that angular distributions are prominently governed by selection rules resulting from angular momentum and parity, hence the even or oddness of the number of absorbed photons.

The two cases of single and multiphoton absorption discussed here are only the two extreme cases. The region of two and few photon double ionization is experimentally completely unexplored. Experiments for two photon double ionization of Helium will become feasible in the near future at the VUV FEL facilities such as the TESLA Test facility in Hamburg.


## Acknowledgments

We thank H. Giessen, G. Urbasch, H. Roskos , T. Löffler and M. Thomson for collaboration on some of the experiments described here. We thank A. Becker, F. Faisal, and W. Becker for many helpful discussions. This work is supported by DFG, BMBF, GSI. R.D. acknowledges supported by the Heisenberg-Programm of the DFG. R.M. B.F. and J.U. acknowledge support by the Leibniz-Programm of the DFG is acknowledged. T. W. is grateful for financial support of the Graduiertenförderung des Landes Hessen.


## References


1. M. Göppert-Mayer. *Ann. d. Phys.*, 9:273, 1931.
2. K. Burnett, V.C. Reed, and P.L. Knight. *J. Phys*, B26:561, 1993.
3. M. Protopapas, C.H. Keitel, and P.L. Knight. *Physics Reports*, 60:389, 1997.

4. R. Dörner, V. Mergel, O. Jagutzki, L. Spielberger, J. Ullrich, R. Moshammer, and H. Schmidt-Böcking. *Physics Reports*, 330:96–192, 2000.
5. R. Moshammer, M. Unverzagt, W. Schmitt, J. Ullrich, and H. Schmidt-Böcking. *Nucl. Instr. Meth.*, B 108:425, 1996.
6. Ken-ichi Hino, T. Ishihara, F. Shimizu, N. Toshima, and J.H. McGuire. *Phys. Rev.*, A48:1271, 1993.
7. A. Kheifets, I. Bray, K. Soejima, A. Danjo, K. Okuno, and A. Yagishita. *J. Phys.*, B34:L247, 2001.
8. R. Shingal and C.D. Lin. *J. Phys*, B24:251, 1991.
9. P. Lambropoulos, P. Maragakis, and J. Zhang. *Physics Reports*, 305:203, 1998.
10. R. Dörner, H. Bräuning, J.M. Feagin, V. Mergel, O. Jagutzki, L. Spielberger, T. Vogt, H. Khemliche, M.H. Prior, J. Ullrich, C.L. Cocke, and H. Schmidt-Böcking. *Phys. Rev.*, A57:1074, 1998.
11. F.W. Byron and C.J. Joachain. *Phys. Rev.*, 164:1, 1967.
12. L. Spielberger, O. Jagutzki, R. Dörner, J. Ullrich, U. Meyer, V. Mergel, M. Unverzagt, M. Damrau, T. Vogt, I. Ali, Kh. Khayyat, D. Bahr, H.G. Schmidt, R. Frahm, and H. Schmidt-Böcking. *Phys. Rev. Lett.*, 74:4615, 1995.
13. L. Spielberger, H. Bräuning, A. Muthig, J.Z. Tang, J. Wang, Y. Qui, R. Dörner, O. Jagutzki, Th. Tschentscher, V. Honkimäki, V. Mergel, M. Achler, Th. Weber, Kh. Khayyat, J. Burgdörfer, J. McGuire, and H. Schmidt-Böcking. *Phys. Rev.*, 59:371, 1999.
14. J.A.R. Samson. *Phys. Rev. Lett.*, 65:2863, 1990.
15. M. Yu. Kuchiev. *Sov. Phys.-JETP Lett.*, 45:404, 1987.
16. P.B. Corkum. *Phys. Rev. Lett.*, 71:1994, 1993.
17. K.J. Schafer, Baorui Yang, L.F. DiMauro, and K.C. Kulander. *Phys. Rev. Lett.*, 70:1599, 1993.
18. J.B. Watson, A. Sanpera, D.G. Lappas, P.L. Knight, and K. Burnett. *Phys. Rev. Lett.*, 78:1884, 1997.
19. M. Lein, E.K.U. Gross, and V. Engel. *Phys. Rev. Lett.*, 85:4707, 2000.
20. D.N. Fittinghoff, P.R. Bolton, B. Chang, and K.D. Kulander. *Phys. Rev.*, A49:2174, 1994.
21. B. Witzel, N. A. Papadogiannis, and D. Charalambidis. *Phys. Rev. Lett.*, 85:2268, 2000.
22. R. Lafon, J. L. Chaloupka, B. Sheehy, P. M. Paul, P. Agostini, K.C.Kulander, , and L. F. DiMauro. *Phys. Rev. Lett.*, 86:2762, 2001.
23. Th. Weber, M. Weckenbrock, A. Staudte, L. Spielberger, O. Jagutzki, V. Mergel, G. Urbasch, M. Vollmer, H. Giessen, , and R. Dörner. *J. Phys*, B33(L127), 2000.
24. Th. Weber, M. Weckenbrock, A. Staudte, L. Spielberger, O. Jagutzki, V. Mergel, G. Urbasch, M. Vollmer, H. Giessen, , and R. Dörner. *Phys. Rev. Lett.*, 84:443, 2000.
25. R. Moshammer, B. Feuerstein, W. Schmitt, A. Dorn, C.T. Schöter, J. Ullrich, H. Rottke, C. Trump, M. Wittmann, G. Korn, K. Hoffmann, and W. Sandner. *Phys. Rev. Lett.*, 84:447, 2000.
26. R. Moshammer B. Feuerstein and J. Ullrich. *J. Phys*, B33:L823, 2000.
27. A. Becker and F.H.M. Faisal. *Phys. Rev. Lett.*, 84:3546, 2000.
28. R. Kopold, W. Becker, H. Rottke, and W. Sandner. *Phys. Rev. Lett.*, 85:371, 2000.
29. K. Sacha and B. Eckhardt. *Phys. Rev.*, A63:043414, 2001.

30. L.B. Fu J. Chen, J. Liu and W.M. Zheng. *Phys. Rev.*, 63:011404R, 2000.
31. M. Achler, V. Mergel, L. Spielberger, Y Azuma R. Dörner, and H. Schmidt-Böcking. *J. Phys.*, B34:L965, 2001.
32. B. Bapat, S. Keller, R. Moshammer, R. Mann, and J Ullrich. *J. Phys*, B33:1437, 2000.
33. A. Dorn, A. Kheifets, C. D. Schröter, B. Najjari, C. Höhr, R. Moshammer, and J. Ullrich. *Phys. Rev. Lett*, 86:3755, 2001.
34. Th. Weber, H. Giessen, M. Weckenbrock, A. Staudte, L. Spielberger, O. Jagutzki, V. Mergel, G. Urbasch, M. Vollmer, , and R. Dörner. *Nature*, 404:608, http://www.opticsexpress.org/oearchive/source/30623.htm, 2000.
35. Th. Weber, M. Weckenbrock, A. Staudte, M. Hattass, L. Spielberger, O. Jagutzki, V. Mergel, G. Urbasch H. Böcking, H. Giessen, H. Bräuning, C. Cocke, M. Prior, and R. Dörner. *Optics Express*, 7(9):368, 2001.
36. M. Weckenbrock, M. Hattass, M. Weckenbrock, M. Hattass, A. Czasch, O. Jagutzki, L Schmidt, T. Weber, H. Roskos, T Löffler, M. Thomson, and R. Dörner. *J. Phys*, B34:L449, 2001.
37. B. Feuerstein, R. Moshammer, D. Fischer, A. Dorn, C. D. Schröter, J. Deipenwisch, J. R. Crespo Lopez-Urrutia, C. Höhr, P. Neumayer, J. Ullrich, H. Rottke, C. Trump, M. Wittmann, G. Korn, , and W. Sandner. *Phys. Rev. Lett.*, 87:043003, 2001.
38. S.P. Goreslavskii and S.V. Popruzhenko. *Optics Express*, 8:395, http://www.opticsexpress.org/oearchive/source/30694.htm, 2001.
39. S.P. Goreslavskii and S.V. Popruzhenko. *J. Phys*, B34:L239, 2001.
40. A. Becker and F.H.M. Faisal. *Phys. Rev.*, A50:3256, 1994.